

Structural features of small RNA precursors determine Argonaute loading in *Caenorhabditis elegans*

Florian A Steiner¹, Suzanne W Hoogstrate¹, Kristy L Okihara¹, Karen L Thijssen^{1,2}, Rene F Ketting¹, Ronald H A Plasterk¹ & Titia Sijen^{1,2}

In *C. elegans*, DCR-1 is required for the maturation of both short interfering RNAs (siRNAs) and microRNAs (miRNAs), which are subsequently loaded into different Argonaute proteins to mediate silencing via distinct mechanisms. We used *in vivo* analyses to show that precursors of small RNAs contain structural features that direct the small RNAs into the RNA interference (RNAi) pathway or the miRNA-processing pathway. Nucleotide changes in the pre-let-7 miRNA precursor that make its stem fully complementary cause the resulting small RNA to be recognized as siRNA and induce binding to RDE-1, which leads to RNAi. Mismatches of 1 to 3 nucleotides at various positions in the stem of the precursor restore direction into the miRNA pathway, as the largest portion of such small RNA variants is associated with ALG-1. The Argonaute proteins to which the small RNAs are bound determine the silencing mode, and no functional overlap between RDE-1 and ALG-1 was detected.

miRNAs and siRNAs were discovered independently as guide molecules in different silencing mechanisms^{1,2}. siRNAs function in the RNAi pathway that is usually induced by long double-stranded RNA (dsRNA)¹, whereas miRNAs are endogenously expressed and processed from hairpin precursors^{3,4}. The small RNAs in both pathways function through binding to Argonaute proteins, and the production of each requires a Dicer protein family member^{5,6}. Dicers are multi-domain proteins containing two RNase III-like domains that are used to cut precursor (pre)-miRNAs and dsRNAs into small RNA duplexes with 2-nucleotide 3' overhangs^{7,8}. The strand of the small-RNA duplex that is preserved to mediate silencing is called the guide strand or miRNA*, and the strand that is discarded is called the passenger strand or miRNA* (ref. 9). pre-miRNAs are derived from long endogenous transcripts that are processed in the nucleus by the enzyme Drosha^{10,11} and subsequently exported to the cytoplasm as substrates for Dicer processing^{12,13}. siRNAs are produced by Dicer from long dsRNAs in the cytoplasm⁵. Whereas flies and plants have separate Dicer genes for miRNA and siRNA production^{14–17}, there is only one Dicer gene in *C. elegans*, which is required for both pathways^{18,19}, raising the question of how the two pathways are separated from the dicing step onward. As in other organisms, there are separate Argonaute proteins that bind the different classes of small RNAs: RDE-1 is required for RNAi²⁰, whereas ALG-1 and ALG-2 are required for miRNA-mediated silencing¹⁸. These Argonaute proteins induce different downstream processes. RDE-1 recruits amplification machinery (including an RNA-directed RNA polymerase) to generate secondary siRNAs²¹, which are bound by secondary Argonautes, leading to efficient downregulation of the

target messenger RNA²². miRNAs silence target mRNAs by binding imperfect target sites in the 3' untranslated region and act through various mechanisms, including translation inhibition and deadenylation^{23–25}.

Dicing and subsequent Argonaute loading is well understood in *Drosophila melanogaster*. There are separate Dicer genes for the RNAi and miRNA pathways, and each Dicer protein has a specific dsRNA-binding protein partner: R2D2 interacts with Dicer-2 and functions in the RNAi pathway²⁶, which also depends on Ago2 (refs. 27,28), whereas Loquacious interacts with Dicer-1 and is required, along with Ago1, for miRNA-mediated silencing^{29–31}.

In *C. elegans*, pathway separation is likely to be different, as RNAi and the miRNA pathway converge on DCR-1 and diverge after the dicing step, when the small RNAs are loaded into different Argonaute proteins. RDE-4 is the only characterized homolog of R2D2 and Loquacious in *C. elegans*. It is a dsRNA-binding protein that is required only for RNAi, and not for the miRNA-processing pathway, and interacts with DCR-1 and RDE-1 (ref. 32). RDE-4 has a binding preference for long dsRNA and hardly binds siRNA duplexes³³. RNAi in *C. elegans* is usually induced by long dsRNA, and it has been speculated that RDE-4 recruits DCR-1 to the long dsRNA and directs the diced siRNAs into RDE-1.

We have recently shown that a single siRNA expressed from a *let-7*-derived transgene can induce silencing of the *unc-22* endogenous gene if the siRNA has full complementarity to the target³⁴. The processing of primary and precursor sequences of this transgenic siRNA (termed 22siRNA) is identical to that of an miRNA, but the induced silencing shows the properties of RNAi, as it is dependent on

¹Hubrecht Institute, Koninklijke Nederlandse Akademie van Wetenschappen, Utrecht, 3584 CT, The Netherlands. ²Present addresses: University Medical Center Groningen, Groningen, 9700 RB, The Netherlands (K.L.T.) and Netherlands Forensic Institute, The Hague, 2497 GB, The Netherlands (T.S.). Correspondence should be addressed to T.S. (t.sijen@nfi.minjus.nl) or F.A.S. (f.steiner@niob.knaw.nl).

Received 4 April; accepted 4 September; published online 23 September 2007; doi:10.1038/nsmb1308

rde-1 and *rde-4*, and not on *alg-1* and *alg-2*. It previously remained unclear what directs this small RNA into the RNAi pathway, while the *let-7* miRNA follows the miRNA pathway. Indeed, only 27 of the 969 nucleotides of the primary *let-7* transcript (pri-*let-7*) were changed to obtain pri-22siRNA. The main difference between 22siRNA and miRNAs lies in the stem of the precursor hairpin, which fully matches in pre-22siRNA but contains mismatches in the pre-miRNAs.

Here we use *C. elegans* as an *in vivo* system to analyze the influence of the structures of miRNA and siRNA precursors on Argonaute association. We show that the introduction of a 1- to 3-nucleotide mismatch in the stem of pre-22siRNA at least partly restores recognition as an miRNA and directs the resulting mature small RNA into a different, larger protein complex than that associated with the original 22siRNA. Capture assays and co-immunoprecipitation of RNA with the Argonaute proteins show that small RNAs produced from mismatched precursors are no longer efficiently bound by RDE-1, but rather are bound by ALG-1. These results show that there are specific features in the pre-siRNA or pre-miRNA that direct the mature small RNA, via differential Argonaute loading, into one or the other pathway. We find that the criteria for loading are not strict, as in some cases low levels of small RNAs derived from mismatched precursors are loaded into RDE-1 to mediate RNAi. After the loading step, small RNAs associated with different Argonaute proteins have nonoverlapping functions, and RNAi depends solely on RDE-1, whereas miRNA-mediated silencing does not depend on RDE-1.

RESULTS

Precursors with fully complementary and mismatched stems

To obtain a nematode line expressing a single siRNA, we altered the *let-7* miRNA sequence within pri-*let-7* to produce an siRNA that fully matches the *unc-22* mRNA (Fig. 1a and Supplementary Fig. 1 online)³⁴. The resulting siRNA (22siRNA) induces *unc-22* silencing via the RNAi pathway and, in contrast to the *let-7* miRNA, is produced from a precursor with a fully matching stem.

As the biogenesis of 22siRNA is identical to that of an miRNA, we were surprised that it is directed into the RNAi pathway and bound by RDE-1. The only difference from miRNAs is the fully matching stem of pre-22siRNA, which contrasts with the mismatched stems of pre-miRNAs. In an attempt to restore miRNA-like properties to 22siRNA and to direct it into the miRNA pathway, we generated pre-22siRNA-derived constructs carrying mismatches (mm) in the passenger strand. The resulting small RNAs are identical to 22siRNA but are processed from precursors with a pre-miRNA-like structure (Fig. 1b). The first three constructs

generated carry a 1-, 2- or 3-nucleotide mismatch in the center of the passenger strand (ps mm10, ps mm10–11 and ps mm9–11). To obtain a small RNA precursor with asymmetrical distribution of the mismatches (as seen in most miRNAs), we generated a fourth construct carrying the 3-nucleotide mismatch in the passenger strand at positions 3–5 (ps mm3–5).

To exclude effects of the mature small RNA sequence, we generated constructs that are processed into small RNAs differing from the original 22siRNA by three nucleotides (Fig. 1c). The changed small RNA is processed either from a precursor with a fully complementary stem (balanced mm) or from a mismatched precursor (gs mm10–12). The nucleotide changes also result in a 3-nucleotide bulge of the mature small RNA when it is paired with the *unc-22* target mRNA at the potential cleavage site for the RNA-induced silencing complex (RISC). The ‘balanced mm’ construct has been used previously to show that an siRNA with a 3-nucleotide bulge relative to the target is unable to induce transitive RNAi³⁴.

All the transgenes we studied express small RNAs with the expected sequence and the expected length of 22 nucleotides, as shown by primer-extension analysis (Fig. 1d), indicating that the changes in the precursors do not interfere with folding or correct processing by Drosha and Dicer. To our surprise, we found that expression of these small RNAs does not strictly follow the asymmetry rules for RISC loading⁹. For most constructs used in this study, both ends of the siRNA duplex are similarly stable, making it difficult to predict which strand will be preferred for Argonaute loading. For the ps mm3–5 construct, the side of the duplex closer to the loop is expected to be less stable, favoring the passenger strand for loading. However, levels of the passenger strand were below detection for most constructs, including ps mm3–5 (data not shown).

To permit analysis of additional sequence-unrelated small RNAs that are processed from precursors with mismatched stems³⁵, we also

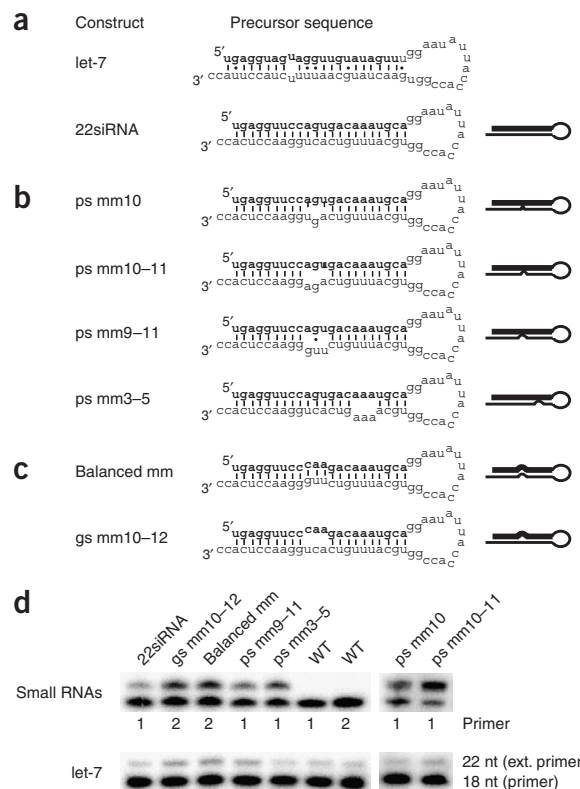


Figure 1 Characteristics of pre-*let-7* and the transgene-derived pre-miRNAs and pre-siRNAs used in this study. (a) Pre-*let-7* and pre-22siRNA. (b) pre-22siRNA-derived precursors producing small RNAs that fully match the *unc-22* mRNA. (c) Precursors producing a small RNA with a 3-nucleotide bulge relative to the *unc-22* mRNA. The constructs were generated by replacing the *let-7* pre-miRNA sequence within the *let-7* primary RNA with the hairpin sequences shown. Transgenes are expressed under control of a *dpy-30* promoter. The bold line in the cartoon of each construct represents the guide strand. (d) The transgenes express correctly processed small RNAs. Small RNAs were detected by primer extension in total RNA. Primer 1 is complementary to the small RNAs derived from the 22siRNA, ps mm9–11, ps mm10–11, ps mm10 and ps mm3–5 precursor constructs. Primer 2 is complementary to the small RNAs derived from the balanced mm and gs mm10–12 constructs. Detection of the miRNA *let-7* was used as a loading control.

Figure 2 Small RNAs derived from mismatched precursors have an miRNA-like distribution in size fractions and fractionate with HA-ALG-1. (a) Detection in wild-type background. (b) Detection in *rde-1*-mutant background. Extracts from lines expressing transgenic small RNAs in WT and *rde-1*-mutant background were fractionated by FPLC, and HA-tagged Argonaute proteins were detected by western blotting (WB). RNA was isolated from fractions, and the guide strands of the small RNAs were detected by primer extension (PE). Vertical lines mark the approximate borders of the siRNA and miRNA peaks. The bold line in the cartoon of each construct represents the guide strand. The samples of each FPLC experiment were run on two gels (separated by white space) simultaneously in the same electrophoresis system.

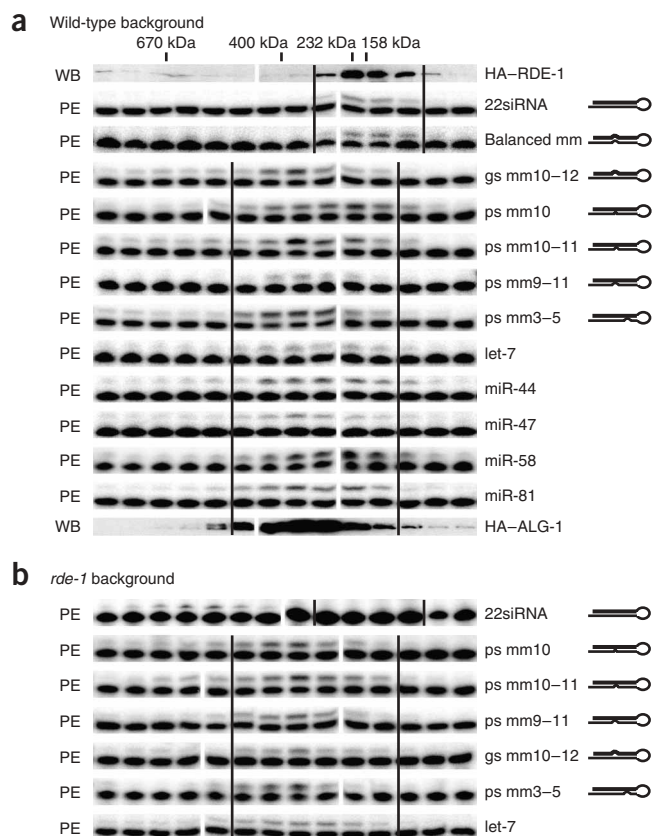
studied endogenous miRNAs (see below). We selected miRNAs with extensive mismatching in their precursor hairpins (miR-42, miR-44, miR-47, miR-58 and miR-81) and miRNAs containing only a single mismatch in their precursors (let-7 and miR-71) (Supplementary Fig. 2 online).

Small RNA precursors influence protein complex formation

To analyze whether the small RNAs are present in specific protein complexes, we used fast protein liquid chromatography (FPLC) to fractionate protein complexes according to size. We isolated RNA from each fraction and detected small RNAs by primer extension using primers specific for the different transgenic small RNAs and five miRNAs (let-7, miR-44, miR-47, miR-58 and miR-81) (Fig. 2a). To enable detection of ALG-1 and RDE-1 by western blotting, we used transgenic lines expressing hemagglutinin (HA)-tagged versions of RDE-1 and ALG-1 (refs. 32,36).

siRNA ribonucleoprotein particles and miRNA ribonucleoprotein particles show different size distributions in this type of analysis^{34,37}. Whereas siRNAs are associated with RDE-1 and reside in a rather narrow peak around 150 kDa, miRNAs are associated with ALG-1 and have a broader distribution that peaks around 250 kDa. Small RNAs processed from perfectly matching precursors (22siRNA and balanced mm) fractionate with HA-RDE-1 in the expected peak of about 150 kDa (Fig. 2a). Small RNAs derived from precursors with mismatches (ps mm10, ps mm10-11, ps mm9-11, ps mm3-5 and gs mm10-12), in contrast, fractionate with HA-ALG-1 rather than with HA-RDE-1, and their size distributions resemble that of an miRNA—for example, let-7, miR-44, miR-47, miR-58 or miR-81 (Fig. 2a). The observed size distribution is independent of the position of the mismatches within the precursor, and a single mismatch is enough to induce a change in the protein-complex association of the small RNA. It remains unclear whether subtle differences in broadness of the peaks between the various mismatched constructs result from differences in expression levels or from differences in the association of the RNAs with protein complexes.

22siRNA is bound by RDE-1, and in an *rde-1* mutant (as in an *rde-4* mutant), it is present in a higher-molecular weight fraction that also contains Dicer activity³⁴. The passenger strand of the 22siRNA duplex, which is usually below detection level, accumulates in these mutants and fractionates with the guide strand, suggesting that the siRNA duplex remains bound to a DCR-1 complex if Argonaute loading is prevented (Supplementary Fig. 3 online). The distributions of small RNAs derived from precursors with mismatches (including the miRNAs analyzed) are affected very little by the *rde-1* knockout (Fig. 2b). There seems to be a subtle shift of the peak away from the fractions where RDE-1 resides, implying that only small amounts of these small RNAs are bound to RDE-1 in the wild-type background. We later confirmed this observation by immunoprecipitation experiments and phenotypic analysis (see below). However, the majority of



each small RNA derived from a mismatched precursor fractionates with ALG-1 in the *rde-1*-mutant background (Fig. 2b).

Argonaute association depends on the precursor structure

To analyze Argonaute association more directly, we crossed a selection of the nematode lines carrying the different small RNA-expressing transgenes (22siRNA, ps mm9-11, balanced mm and gs mm10-12) with the lines expressing HA-tagged versions of RDE-1 or ALG-1 (refs. 32,36). Antibody specific to the HA tag was used to immunoprecipitate the Argonaute protein, RNA was isolated from input extracts, supernatants and immunoprecipitates, and small RNAs were detected by northern blotting (Fig. 3 and Supplementary Fig. 4 online).

Small RNAs processed from precursors with fully matching stems (22siRNA and balanced mm) were precipitated efficiently with RDE-1 but only weakly with ALG-1. Conversely, small RNAs processed from mismatched precursors (including all miRNAs tested) were precipitated efficiently with ALG-1 but only weakly with RDE-1. To compare the binding of different small RNAs, we measured the amounts of each RNA in the empty-bead control supernatants (EB sup) and in the HA immunoprecipitates, and calculated the ratio of the RNA in each immunoprecipitate to the RNA in the EB sup. Small RNAs derived from fully matching precursors were enriched 15- to 30-fold in the RDE-1 immunoprecipitates, in contrast to small RNAs derived from mismatched precursors, which had immunoprecipitate/EB sup ratios of 0.5 to 2. The results were inverted for the ALG-1 immunoprecipitates, although the difference between the matched and mismatched precursors was less pronounced, with ratios of 0.1 to 2 for fully matching precursors and 2.5 to 4.5 for mismatched precursors (similar to miRNAs).

Analysis of endogenous miRNAs indicated that small RNAs derived from precursors with extensive mismatches (miR-42, miR-44, miR-47,

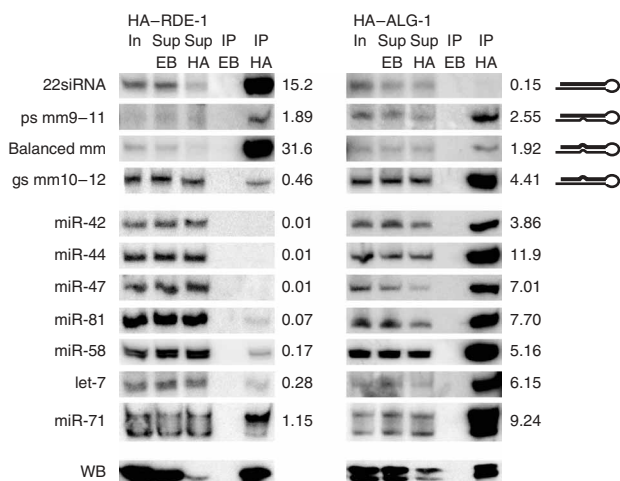


Figure 3 Small RNAs derived from mismatched precursors are bound by ALG-1 rather than RDE-1. HA-RDE-1 or HA-ALG-1 was immunoprecipitated from lines expressing one of the tagged Argonaute proteins and one of the small RNA constructs. HA-tagged Argonaute proteins were detected by western blotting (WB). RNA was isolated from input extracts (In), supernatants (Sup) and immunoprecipitated protein complexes (IP), and small RNAs were detected by northern blotting. The bold line in the cartoon of each construct represents the guide strand. 22siRNA, ps mm9-11, balanced mm, gs mm10-12 and seven endogenous miRNAs were detected in HA-RDE-1 and HA-ALG-1 immunoprecipitates. Immunoprecipitate/EB Sup RNA ratios (see text) are indicated beside blots. Equal amounts of input extract or RNA and supernatant extract or RNA were loaded. Approximately equal amounts of HA-tagged protein were loaded for western blots of input and immunoprecipitates (for example, 10 μ l input extract and immunoprecipitate from 10 μ l extract). In northern blots, HA-tagged proteins were enriched about 40-fold in the immunoprecipitates compared to the input and supernatants (for example, RNA from 25 μ l input and supernatant extracts and RNA from immunoprecipitate from 1 ml extracts). HA, HA-RDE-1 or HA-ALG-1; EB, empty-bead control.

miR-81 and miR-58) are only weakly bound by HA-RDE-1 (ratios of 0.01–0.17), whereas miRNAs with only few mismatches (let-7 and miR-71) are more strongly associated with RDE-1 (ratios of 0.25 and 1.2). Thus, the extent of the mismatches in the precursor apparently influenced the Argonaute loading of endogenous miRNAs as well as our small-RNA constructs. However, the amounts of miRNAs associated with RDE-1 never reached the levels precipitated with ALG-1, confirming that small RNAs derived from precursors with mismatches enter mainly the miRNA pathway.

To validate these findings using a second approach, we captured Argonaute proteins using biotinylated 2'-O-methyloligonucleotides complementary to either 22siRNA, the gs mm10-12 small RNA, the let-7 miRNA or an unrelated RNA (encoding luciferase GL3). Argonaute proteins were detected by western blotting. Whereas HA-RDE-1 is efficiently captured by 22siRNA and the balanced mm small RNAs (Fig. 4). This confirms that the majority of the RNAs are bound to HA-RDE-1 only in the case of the small RNAs processed from precursors with fully matching stems (22siRNA and balanced mm); in contrast, constructs processed from mismatched precursors (gs mm10-12 and ps mm9-11) are bound to RDE-1 only in small amounts. Unfortunately, capture assays involving ALG-1 were not conclusive, because HA-ALG-1 interacted with the 22siRNA capture oligonucleotide even in the absence of small RNA-expressing transgenes (data not shown). Most probably, let-7-ALG-1 complexes can bind the 22siRNA capture oligonucleotide because it differs by only a few nucleotides from a perfect let-7 target, owing to the design of the construct. Apparently, a few mismatches between the small RNA and the 2'-O-methyloligonucleotide do not interfere with the capture. Nevertheless, the results from the RDE-1 capture assays confirm the findings from the RNA immunoprecipitation experiments and strengthen the finding that small RNAs processed from precursors with fully matching stems are recognized as siRNAs and directed into the RNAi pathway.

Requirements for RNAi induction

The 22siRNA sequence was designed to fully match a single target site in the *unc-22* mRNA, and it induces *unc-22* silencing through association with RDE-1 and the generation of secondary siRNAs, resulting in a twitching phenotype of the nematodes³⁴. Small RNAs that have sequences identical to 22siRNA, but are processed from mismatched precursors, reside in differently sized protein complexes and are associated mainly with ALG-1 (Figs. 2 and 3). To our surprise,

the constructs with a central mismatch in the passenger strand (ps mm10, ps mm10-11 and ps mm9-11) also induce a twitching phenotype. To analyze whether the *unc-22*-silencing phenotype is achieved through the RNAi pathway, we crossed these strains with an RNAi-deficient strain carrying an early stop mutation in the *rde-1* gene. We found that in all cases the *unc-22*-silencing phenotype is entirely dependent on *rde-1*, and thus on the RNAi pathway, and cannot be achieved through the miRNA pathway. Although the small RNAs derived from the ps mm10, ps mm10-11 and ps mm9-11 precursors resemble miRNAs in size fractions and the majority of these small RNAs are loaded into ALG-1, small amounts are also directed into RDE-1 to mediate silencing via RNAi. This is also reflected by the finding that little of the ps mm9-11 small RNA is bound to HA-RDE-1 (Fig. 3).

Three conclusions can be drawn from these findings. First, small RNAs processed from mismatched precursors are bound mainly by an miRNA ribonucleoprotein-like complex. Second, loading criteria are not strict, and the same construct can feed into both the RNAi and miRNA pathways. Third, once small RNAs are loaded into Argonaute proteins, no functional redundancy between RDE-1 and ALG-1 is evident. This is indicated by the observation that in the absence of RDE-1, the ps mm10, ps mm10-11 and ps mm9-11 constructs are unable to induce the *unc-22*-silencing phenotype even though substantial amounts are still present in the miRNA-like complex, most probably bound to ALG-1 (Fig. 2). As expected, secondary siRNAs

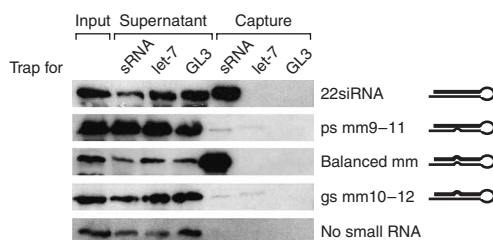


Figure 4 RDE-1 is associated mainly with small RNAs derived from fully matching precursors. HA-RDE-1–small RNA complexes were captured with biotinylated 2'-O-methyloligonucleotides complementary to the small RNAs and pulled down using streptavidin beads. HA-RDE-1 was detected by western blotting. Capture oligonucleotides are perfect antisense matches to let-7 miRNA, an unrelated luciferase GL3 sequence, 22siRNA, or gs mm10-12. The captured fractions were enriched about five-fold in immunoprecipitates compared to input and supernatant.

were observed only in lines with an *unc-22*-silencing phenotype (Supplementary Fig. 5 online), confirming that an siRNA amplification step is required to achieve RNAi. The ps mm9–11 small RNA is bound to HA–RDE-1 in small amounts compared to 22siRNA (Figs. 3 and 4), yet the abundance of secondary siRNAs and the penetrance of the phenotype are comparable. Apparently, these small amounts of RNA are sufficient to trigger RNAi amplification and result in robust silencing. We cannot exclude the possibility that there is a low level of ALG-1-mediated targeting of the *unc-22* mRNA. However, if present, this does not produce a visible *unc-22*-silencing phenotype, most probably because miRNA-mediated silencing is not an amplified process and because a single target site within the coding sequence is not sufficient to induce miRNA-mediated silencing.

Notably, the ps mm3–5 construct does not induce an *unc-22*-silencing phenotype, although it gives rise to a small RNA identical to 22siRNA. The asymmetric structure of the stem of this precursor probably is a better substrate for the miRNA pathway and does not induce loading into RDE-1. However, we do not have sufficient data for a generalized conclusion about the effects of mismatch positions within the precursor.

The small RNAs that contain a mismatch to the target mRNA (balanced mm and gs mm10–12) do not induce an *unc-22*-silencing phenotype, even in the case of a small RNA processed from a precursor that has a fully base-pairing stem and is associated with RDE-1 (balanced mm). However, they follow the Argonaute-loading rules observed for all 22siRNA derivatives: RDE-1 association when processed from a fully matching precursor, and ALG-1 association when processed from a mismatched precursor (Figs. 2–4).

In summary, phenotypic analysis of the lines carrying the different precursor constructs indicates that RNAi is induced only by small RNAs that have perfect complementarity to the target and a precursor structure that induces loading into RDE-1.

DISCUSSION

In *C. elegans*, the miRNA-processing pathway and the siRNA-processing (RNAi) pathway share a single Dicer gene¹⁹, raising the question of how small RNAs processed by the same enzyme end up in separate pathways. siRNA processed from a miRNA-like precursor can trigger an RNAi response, so the regulatory mechanism is more subtle than a simple distinction between the long dsRNAs that trigger RNAi and the hairpin precursors that trigger miRNA processing. A few nucleotide changes in a pre-miRNA to make the stem fully complementary are sufficient to direct the resulting small RNA into the RNAi instead of the miRNA pathway, indicating that the structure of the precursor affects Argonaute loading.

Here we show that a small RNA is directed into the RNAi pathway as long as the stem of the hairpin precursor fully matches. If there is a 1-, 2- or 3-nucleotide mismatch in the stem of the precursor hairpin, the resulting small RNAs are recognized as miRNAs and preferentially loaded into ALG-1. However, this distinction is not absolute, and there are intermediate cases. The ps mm10, ps mm10–11 and ps mm9–11 constructs analyzed in this study seem to have properties that direct the small RNAs into Argonautes of both pathways, as these constructs show an miRNA-like distribution in size fractions (Fig. 2) but still induce silencing through binding to RDE-1 (Fig. 3). The gs mm10–12 small RNA is equally symmetrical and is also weakly bound to HA–RDE-1 (Fig. 3), but it cannot induce a silencing phenotype because of the mismatch to the target sequence. Similarly, let-7 and miR-71 are endogenous miRNAs that are associated not only with ALG-1, but also, in small amounts, with RDE-1 (Fig. 3). These small RNAs might still partly be recognized as siRNAs because their

precursors carry mismatches in the center, but the ends of the processed small RNA duplex are fully base-pairing. The symmetry of a central mismatch and fully matching ends is abolished in the precursor of the ps mm3–5 construct. This might prevent the small RNA from being partly recognized as an siRNA, which may be the reason it does not induce an *unc-22*-silencing phenotype (note that the mature small RNA processed from the ps mm3–5 precursor is identical to that processed from the ps mm9–11 precursor). These findings suggest that the presence of a mismatch and its position within the small RNA precursor affect Argonaute loading and fine-tune the distribution of RNAs between the RNAi and miRNA pathways. The extent to which other Argonaute proteins are involved in binding unassigned small RNAs is difficult to assess, because the precise function of many Argonautes (and therefore the readout of fortuitous Argonaute loading) is not known, and because there is redundancy between some Argonaute family members²².

Downstream of Argonaute loading, however, we find that the miRNA and siRNA pathways are functionally nonredundant. ALG-1 cannot rescue the *rde-1* mutant, even when loaded with the same small RNA, and the *unc-22*-silencing phenotype is dependent on *rde-1* in all cases analyzed (when the phenotype is induced by 22siRNA, ps mm10, ps mm10–11 or ps mm9–11). In contrast, RDE-1 does not seem to have any role in miRNA-mediated silencing, as RDE-1 cannot rescue the function of ALG-1 in the miRNA pathway in the *alg-1* mutant¹⁸, and the *rde-1* mutant has no abnormal phenotype except deficiencies in RNAi²⁰ and virus resistance^{38,39}. Also, the size distribution of miRNA-containing complexes is hardly affected by the *rde-1* mutation (Fig. 2b).

Because identical small RNAs can be directed into different pathways, cells need a second layer of safeguards against off-target effects—especially against unintended RNAi, which is an amplified process. Once an siRNA is loaded into RDE-1, its ability to silence a target requires full complementarity to its target. A single mismatch greatly reduces silencing, and a 3-nucleotide bulge completely abolishes it³⁴. These strict requirements for target recognition might serve as a safeguard against off-target effects of ‘misdirected’ small RNAs. The extent to which miRNAs are loaded into RDE-1 *in vivo* has yet to be systematically analyzed, but the finding that detectable amounts of miR-71, let-7, miR-58 and miR-81 are present in HA–RDE-1 immunoprecipitates (Fig. 3) suggests that this is not uncommon. Whether the association of these miRNAs with RDE-1 is biologically relevant remains to be investigated. As the endogenous role of RDE-1 is largely unknown, it is difficult to speculate which classes of small RNAs are bound to RDE-1 in the absence of an RNAi trigger. RNAi is usually an artificially induced process, and its natural role most probably is to protect the nematodes against viruses^{38–40}. To achieve this, it is possible that RDE-1 binds a large set of small RNAs from various origins and searches for perfectly matching targets to ensure recognition of small RNAs derived from viral genomes and an efficient antiviral response. If small RNAs from various origins (including miRNAs) are regularly bound by RDE-1, there is strong evolutionary pressure to prevent unintended, amplified RNAi by maintaining strict target-matching requirements for RNAi. There might be a major risk of unintended RNAi targeting newly evolving miRNAs, for which Argonaute loading as well as target sites are not yet defined.

Several options can be envisioned for achieving differential Argonaute loading. Some uncharacterized machinery may detect the structure of the small RNA precursor and recruit the appropriate Argonaute–Dicer complex. Alternatively, the machinery may assess the small-RNA duplex after dicing and may be directly involved in Argonaute loading. It remains unclear whether Argonaute proteins

themselves can perform such a scanning step, or which other protein factor(s) might participate in this recognition and recruiting or loading process. Two recent studies have shown that in *Drosophila*, siRNAs and miRNAs are sorted into Ago1 and Ago2 by a mechanism that is independent of small-RNA processing by Dcr-1 and Dcr-2 (refs. 41,42). The sorting of siRNA and miRNA reflects the structure of the double-stranded assembly intermediates, in a manner similar to what we describe for the *C. elegans* model in this study. The Dcr-2–R2D2 complex shows a binding preference for small RNAs with fully matching duplexes and promotes their loading into Ago2. A separate mechanism favors the loading of small RNAs from mismatched duplexes into Ago1 (ref. 41). As in *C. elegans*, the Ago1 and Ago2 complexes silence their target RNAs by different mechanisms⁴². The dsRNA-binding protein RDE-4 is the only *C. elegans* homolog of the *Drosophila* R2D2 protein. It is required only for the production and function of siRNA, and not miRNA, and has been implicated in loading of siRNAs into RISC³². We have previously shown that RDE-4 is not required for 22siRNA maturation, but that in the *rde-4* mutant, the mature 22siRNA-containing complex is no longer formed (**Supplementary Fig. 3**)³⁴. The *C. elegans* DCR-1–RDE-4 heterodimer might thus have a function similar to that of the Dcr-2–R2D2 heterodimer in *Drosophila*, recruiting siRNAs to the RNAi pathway by preferentially binding hairpin precursors with perfectly matching stems. However, RDE-4 has a low binding affinity for short dsRNA³³, and its exact role in the loading step therefore remains elusive.

The RNAi and the miRNA pathways might not be the only small RNA pathways that intersect at DCR-1. DCR-1 is required for the production of endogenous siRNAs (endo-siRNAs)⁴³, and several proteins involved in the endogenous RNAi pathway have been found to be associated with DCR-1 (ref. 44). The Argonaute protein ERGO-1 is required for endo-siRNA production and has been proposed to bind primary endo-siRNAs²². However, ERGO-1 has not been described as a DCR-1 interaction partner, whereas ALG-1 and RDE-1 do bind DCR-1 (**Supplementary Fig. 6** online)⁴⁴.

There are several other classes of small RNAs in *C. elegans*, and the biogenesis of most is not well understood. It is therefore difficult to even speculate about how they are directed to the appropriate Argonautes. Several recent studies of novel classes of small RNAs suggest that there is, in many cases, no dicing event in the biogenesis of these molecules; examples include *C. elegans* secondary siRNAs^{34,45} and 21U-RNAs⁴⁶, and *Drosophila* and zebrafish PIWI-interacting RNAs (piRNAs)^{47,48}. These novel classes of small RNAs might therefore require Argonaute-loading machinery that is substantially different from the machinery that loads siRNAs and miRNAs into RDE-1 and ALG-1. If RDE-1 indeed acts as a safeguard against molecular parasites and binds a broad variety of small RNAs, it will be interesting to find out whether RDE-1 binds only small RNAs produced by Dicer, or whether non-diced small RNAs can also be loaded into RDE-1.

The pathways involving small RNAs in *C. elegans* form a complex silencing network, and researchers are only beginning to understand how the different pathways are related to each other, where they overlap and by what mechanisms they are separated. We have found that the degree of complementarity in the hairpin precursor separates the miRNA and siRNA pathways. Small-RNA precursor structures can thus be important in determining the fates of the small RNAs and influence the choice of the silencing modes in which they function.

METHODS

Nematode strains and transgenic lines. The Bristol strain N2 was used as the standard wild-type strain. The alleles used in this study were *rde-1(pk3301)*, *rde-1(ne300)* rescued with *rde-1::HA;rde-4::FLAG*³², *alg-1::HA(pkIs2250)*³⁶,

rde-4(pk301), *unc-119 (ed3)*, 22siRNA(*pkIs2289*), balanced mm(*pkIs2344*), *rde-1 (ne300)* rescued with *rde-1::HA;rde-4::FLAG* crossed with 22siRNA(*pkIs2289*)³⁴.

The small RNA expression vectors are derived from the *unc-119* rescue vector pRP2512. A *dpy-30* promoter (nucleotides (–727) to (–1) of *dpy-30*, numbered relative to ATG in genomic sequence) drives expression of the primary *let-7* miRNA sequence (genomic nucleotide positions X:14744399 to X:14743431), in which the BamHI–BstBI region is replaced by a sequence encoding a pre-miRNA or pre-siRNA. This sequence was generated by annealing two oligonucleotides to create a fragment with BamHI and BstBI overhangs. Forward primer sequences for various constructs are as follows: gs mm10–12, 5'-GATCCGGTGAGGTTCCCAAGACAAATGCAGGAATATTAC CACCGGTGCATTTGTCAGTGGAACTCACC GGAGACAGA AACTCTT-3'; ps mm10, 5'-GATCCGGTGAGGTTCCAGTGACAAATGCAGGAATATTACCACC GGTGCATTTGTCAGTGGAACTCACC GGAGACAGA AACTCTT-3'; ps mm 10–11, 5'-GATCCGGTGAGGTTCCAGTGACAAATGCAGGAATATTACCACC GGTGCATTTGTCAGAGGAACCTCACC GGAGACAGA AACTCTT-3'; ps mm 9–11, 5'-GATCCGGTGAGGTTCCAGTGACAAATGCAGGAATATTACCACC GTGCATTTGTCAGAGGAACCTCACC GGAGACAGA AACTCTT-3'; ps mm3–5, 5'-GATCCGGTGAGGTTCCAGTGACAAATGCAGGAATATTACCACC GGTTCC AAAAGTCACTGGAACCTCACC GGAGACAGA AACTCTT-3' (sequences of reverse primers are available on request). Sequences for 22siRNA and the balanced mm construct have been described³⁴. Transgenic lines were generated using standard ballistic transformation in *unc119(ed3)* nematodes.

Newly generated alleles are ps mm10(*pkIs2450*), ps mm10–11(*pkIs2451*), ps mm9–11(*pkIs2432*, *pkIs2446*), ps mm3–5(*pkIs2438*, *pkIs2531*), balanced mm(*pkIs2441*), and gs mm10–12(*pkIs2291*). The small RNAs from the various constructs target nucleotides 11925–11946 of the *unc-22* spliced sequence.

rde-1(ne300) rescued with *rde-1::HA;rde-4::FLAG* was crossed to balanced mm(*pkIs2441*), gs mm10–12(*pkIs2291*) and ps mm9–11(*pkIs 2432*). *alg-1::HA(pkIs2250)* was crossed to 22siRNA22(*pkIs2289*), balanced mm(*pkIs2441*), gs mm10–12(*pkIs2291*) and ps mm9–11(*pkIs 2432*).

Nematodes were cultured according to standard procedures, and the twitching phenotype associated with *unc-22* silencing was detected by eye and confirmed in 1% (w/v) nicotine. *unc-22* nematodes are resistant to nicotine, making their twitching phenotype obvious compared to the WT animals, which are paralyzed by nicotine.

Protein assays. Nematode extracts were prepared in FPLC buffer (150 mM NaCl, 10 mM Tris-HCl (pH 7.5), 5 mM MgCl₂, 2 mM CaCl₂, 2 mM DTT, 0.2% (v/v) Nonidet P-40 substitute, 5% (v/v) glycerol and one tablet of complete mini-EDTA-free protease inhibitor cocktail (Roche) per 10 ml buffer) and size-fractionated into 500- μ l fractions using a Superdex200 column (Amersham) as described³⁷. HA–RDE-1 and HA–ALG-1 were analyzed by western blotting according to standard procedures using anti-HA 3F10 (Roche).

For capture assays, nematode extracts were prepared in CAPT buffer (10 mM Tris-HCl (pH 7.5), 100 mM KCl, 2 mM MgCl₂, 0.5% (v/v) Nonidet P-40 substitute, 15% (v/v) glycerol, 5 mM DTT and one tablet of complete mini-EDTA-free protease inhibitor cocktail (Roche) per 10 ml buffer). Extracts were incubated for 1 h at room temperature with 10 pmol 31-nucleotide 2'-O-methyloligonucleotides with a 5' biotin group. HA-tagged Argonaute proteins were pulled down using 25 μ l Streptavidin Dynabeads. After three washes in CAPT buffer, HA–RDE-1 and HA–ALG-1 were analyzed by western blotting according to standard procedures using anti-HA 3F10 (Roche). The 2'-O-methyloligonucleotide sequences are 5'-UUUC-X-AUCAC-3', X being the sequence antisense to that of 22siRNA, the gs mm 10–12 small RNA, the *let-7* miRNA or the luciferase sequence 5'-UCGAAGUACUCAGCGUAAGUU-3'.

For RNA immunoprecipitations, HA–ALG-1 and HA–RDE-1 were immunoprecipitated from nematode extract prepared in immunoprecipitation buffer (10 mM Tris-HCl (pH 7.5), 100 mM KCl, 2 mM MgCl₂, 0.05% (v/v) Tween-20, 15% (v/v) glycerol, 5 mM DTT and 1 tablet of complete mini-EDTA-free protease inhibitor cocktail (Roche) per 10 ml buffer) and incubated 2 h at 4 °C with anti-HA 3F10 affinity matrix (Roche). Protein G-agarose (Roche) was used as the 'empty-bead' control. After five washes with immunoprecipitation buffer, HA–RDE-1 and HA–ALG-1 were analyzed by western blotting according to standard procedures using anti-HA 3F10 (Roche).

RNA analysis. RNA from nematode extracts, FPLC fractions and RNA immunoprecipitations was isolated using Trizol LS (Invitrogen) according to

the manufacturer's protocol. Low-molecular weight RNA of nematodes was prepared using the miRvana miRNA Isolation Kit (Ambion) according to the manufacturer's protocol. RNase protection assays were performed as described³⁴, with a probe targeting nucleotides 11432–11924 of the spliced *unc-22* mRNA, upstream of the 22siRNA target site.

Primer-extension reactions were performed using 0.4 μ l (200 U μ l⁻¹) M-MLV-Reverse transcriptase (Promega) and a 5' end-labeled 18-nucleotide DNA sequence purified on a G25-column (GE Healthcare). Sequences were 5'-TGCATTTGCTCACTGGAAC-3' for the guide strands of 22siRNA, ps mm3–5 and ps mm9–11; 5'-TGCATTTGCTTGGGAAC-3' for the guide strands of gs mm10–12 and balanced mm; 5'-GGTACAGTTCCAGTGAC-3' for the passenger strand of 22siRNA; 5'-AACTATACAACCTACTAC-3' for let-7; 5'-AGCTGAATGTGTCTC-3' for miR-44; 5'-TGAAGAGAGCGCCTCC-3' for miR-47; 5'-ATTGCCGTACTGAACGAT-3' for miR-58; and 5'-ACTAGCTTTACAGATG-3' for miR-81. RNA and oligonucleotide were denatured at 83 °C for 5 min and annealed at 48 °C for 5 min, after which reverse transcriptase-containing reaction mixture was added and the reaction mixture was incubated for 2 h at 48 °C. After denaturation at 99 °C for 1 min, samples were analyzed on 15% (w/v) polyacrylamide-urea gels using standard procedures.

For northern blotting analyses, RNA was separated on 15% (w/v) polyacrylamide-urea gels and blotted according to standard procedures. Transgenic small RNAs, let-7 and miR-58 were detected using locked nucleic acid (LNA) probes; miR-42, miR-44, miR-47, miR-71 and miR-81 were detected using DNA probes. Blots were prehybridized for 30 min in hybridization buffer (0.36 M Na₂HPO₄, 0.14 M NaH₂PO₄, 1 mM EDTA, 7% (w/v) SDS) and hybridized overnight in hybridization buffer containing 10 pM 5' end-labeled probe. LNA probes were hybridized at 60 °C, DNA probes at 37 °C. After two stringency washes of 30 min each (at 50 °C in 1 \times SSC and 0.1% (w/v) SDS for LNA probes, and at 37 °C in 2 \times SSC and 0.1% (w/v) SDS for DNA probes) the signal was detected by phosphorimaging according to standard procedures. The intensities of the signals were quantified using ImageQuant 5.2 (Molecular Dynamics).

Note: Supplementary information is available on the Nature Structural & Molecular Biology website.

ACKNOWLEDGMENTS

We thank G. Hannon and F. Rivas (Cold Spring Harbor Laboratory) for providing reagents and help with the capture assays, B. Tops (Hubrecht Institute) and C. Mello (University of Massachusetts Medical School) for providing strains and W. Kloosterman for discussions and critical reading of the manuscript. This work was supported by a Vidi fellowship from the Dutch Scientific Organization (NWO) to T.S. and a European Union grant (HPRN-CT-2002-00257) and Netherlands Genomics Initiative grant (050-72-415) to F.A.S.

AUTHOR CONTRIBUTIONS

F.A.S., S.W.H., K.L.O., K.L.T. and T.S. carried out experiments; T.S., F.A.S., R.F.K. and R.H.A.P. supervised the research; F.A.S. and T.S. wrote the paper.

Published online at <http://www.nature.com/nsmb/>

Reprints and permissions information is available online at <http://npg.nature.com/reprintsandpermissions>

1. Fire, A. *et al.* Potent and specific genetic interference by double-stranded RNA in *Caenorhabditis elegans*. *Nature* **391**, 806–811 (1998).
2. Lee, R.C., Feinbaum, R.L. & Ambros, V. The *C. elegans* heterochronic gene *lin-4* encodes small RNAs with antisense complementarity to *lin-14*. *Cell* **75**, 843–854 (1993).
3. Bartel, D.P. MicroRNAs: genomics, biogenesis, mechanism, and function. *Cell* **116**, 281–297 (2004).
4. Kim, V.N. Small RNAs: classification, biogenesis, and function. *Mol. Cells* **19**, 1–15 (2005).
5. Bernstein, E., Caudy, A.A., Hammond, S.M. & Hannon, G.J. Role for a bidentate ribonuclease in the initiation step of RNA interference. *Nature* **409**, 363–366 (2001).
6. Hutvagner, G. *et al.* A cellular function for the RNA-interference enzyme Dicer in the maturation of the let-7 small temporal RNA. *Science* **293**, 834–838 (2001).
7. Zhang, H., Kolb, F.A., Brondani, V., Billy, E. & Filipowicz, W. Human Dicer preferentially cleaves dsRNAs at their termini without a requirement for ATP. *EMBO J.* **21**, 5875–5885 (2002).
8. Zhang, H., Kolb, F.A., Jaskiewicz, L., Westhof, E. & Filipowicz, W. Single processing center models for human Dicer and bacterial RNase III. *Cell* **118**, 57–68 (2004).
9. Schwarz, D.S. *et al.* Asymmetry in the assembly of the RNAi enzyme complex. *Cell* **115**, 199–208 (2003).
10. Lee, Y., Jeon, K., Lee, J.T., Kim, S. & Kim, V.N. MicroRNA maturation: stepwise processing and subcellular localization. *EMBO J.* **21**, 4663–4670 (2002).

11. Lee, Y. *et al.* The nuclear RNase III Drosha initiates microRNA processing. *Nature* **425**, 415–419 (2003).
12. Yi, R., Qin, Y., Macara, I.G. & Cullen, B.R. Exportin-5 mediates the nuclear export of pre-microRNAs and short hairpin RNAs. *Genes Dev.* **17**, 3011–3016 (2003).
13. Lund, E., Guttinger, S., Calado, A., Dahlberg, J.E. & Kutay, U. Nuclear export of microRNA precursors. *Science* **303**, 95–98 (2004).
14. Lee, Y.S. *et al.* Distinct roles for *Drosophila* Dicer-1 and Dicer-2 in the siRNA/miRNA silencing pathways. *Cell* **117**, 69–81 (2004).
15. Xie, Z. *et al.* Genetic and functional diversification of small RNA pathways in plants. *PLoS Biol.* **2**, E104 (2004).
16. Vazquez, F. *Arabidopsis* endogenous small RNAs: highways and byways. *Trends Plant Sci.* **11**, 460–468 (2006).
17. Brodersen, P. & Voinnet, O. The diversity of RNA silencing pathways in plants. *Trends Genet.* **22**, 268–280 (2006).
18. Grishok, A. *et al.* Genes and mechanisms related to RNA interference regulate expression of the small temporal RNAs that control *C. elegans* developmental timing. *Cell* **106**, 23–34 (2001).
19. Ketting, R.F. *et al.* Dicer functions in RNA interference and in synthesis of small RNA involved in developmental timing in *C. elegans*. *Genes Dev.* **15**, 2654–2659 (2001).
20. Tabara, H. *et al.* The *rde-1* gene, RNA interference, and transposon silencing in *C. elegans*. *Cell* **99**, 123–132 (1999).
21. Sijen, T. *et al.* On the role of RNA amplification in dsRNA-triggered gene silencing. *Cell* **107**, 465–476 (2001).
22. Yigit, E. *et al.* Analysis of the *C. elegans* Argonaute family reveals that distinct Argonautes act sequentially during RNAi. *Cell* **127**, 747–757 (2006).
23. Valencia-Sanchez, M.A., Liu, J., Hannon, G.J. & Parker, R. Control of translation and mRNA degradation by miRNAs and siRNAs. *Genes Dev.* **20**, 515–524 (2006).
24. Pillai, R.S. *et al.* Inhibition of translational initiation by Let-7 MicroRNA in human cells. *Science* **309**, 1573–1576 (2005).
25. Pillai, R.S., Bhattacharyya, S.N. & Filipowicz, W. Repression of protein synthesis by miRNAs: how many mechanisms? *Trends Cell Biol.* **17**, 118–126 (2007).
26. Liu, Q. *et al.* R2D2, a bridge between the initiation and effector steps of the *Drosophila* RNAi pathway. *Science* **301**, 1921–1925 (2003).
27. Caudy, A.A. & Hannon, G.J. Induction and biochemical purification of RNA-induced silencing complex from *Drosophila* S2 cells. *Methods Mol. Biol.* **265**, 59–72 (2004).
28. Rand, T.A., Ginalski, K., Grishin, N.V. & Wang, X. Biochemical identification of Argonaute 2 as the sole protein required for RNA-induced silencing complex activity. *Proc. Natl. Acad. Sci. USA* **101**, 14385–14389 (2004).
29. Forstemann, K. *et al.* Normal microRNA maturation and germ-line stem cell maintenance requires Loquacious, a double-stranded RNA-binding domain protein. *PLoS Biol.* **3**, e236 (2005).
30. Saito, K., Ishizuka, A., Siomi, H. & Siomi, M.C. Processing of pre-microRNAs by the Dicer-1-Loquacious complex in *Drosophila* cells. *PLoS Biol.* **3**, e235 (2005).
31. Okamura, K., Ishizuka, A., Siomi, H. & Siomi, M.C. Distinct roles for Argonaute proteins in small RNA-directed RNA cleavage pathways. *Genes Dev.* **18**, 1655–1666 (2004).
32. Tabara, H., Yigit, E., Siomi, H. & Mello, C.C. The dsRNA binding protein RDE-4 interacts with RDE-1, DCR-1, and a DEXH-box helicase to direct RNAi in *C. elegans*. *Cell* **109**, 861–871 (2002).
33. Parker, G.S., Eckert, D.M. & Bass, B.L. RDE-4 preferentially binds long dsRNA and its dimerization is necessary for cleavage of dsRNA to siRNA. *RNA* **12**, 807–818 (2006).
34. Sijen, T., Steiner, F.A., Thijssen, K.L. & Plasterk, R.H. Secondary siRNAs result from unprimed RNA synthesis and form a distinct class. *Science* **315**, 244–247 (2007).
35. Kim, V.N. MicroRNA biogenesis: coordinated cropping and dicing. *Nat. Rev. Mol. Cell Biol.* **6**, 376–385 (2005).
36. Tops, B.B., Plasterk, R.H. & Ketting, R.F. The *Caenorhabditis elegans* Argonautes ALG-1 and ALG-2: almost identical yet different. *Cold Spring Harb. Symp. Quant. Biol.* **71**, 189–194 (2006).
37. Caudy, A.A. *et al.* A micrococcal nuclease homologue in RNAi effector complexes. *Nature* **425**, 411–414 (2003).
38. Lu, R. *et al.* Animal virus replication and RNAi-mediated antiviral silencing in *Caenorhabditis elegans*. *Nature* **436**, 1040–1043 (2005).
39. Wilkins, C. *et al.* RNA interference is an antiviral defence mechanism in *Caenorhabditis elegans*. *Nature* **436**, 1044–1047 (2005).
40. Plasterk, R.H. RNA silencing: the genome's immune system. *Science* **296**, 1263–1265 (2002).
41. Tomari, Y., Du, T. & Zamore, P.D. Sorting of *Drosophila* small silencing RNAs. *Cell* **130**, 299–308 (2007).
42. Forstemann, K., Horwich, M.D., Wee, L., Tomari, Y. & Zamore, P.D. *Drosophila* microRNAs are sorted into functionally distinct argonaute complexes after production by dicer-1. *Cell* **130**, 287–297 (2007).
43. Lee, R.C., Hammell, C.M. & Ambros, V. Interacting endogenous and exogenous RNAi pathways in *Caenorhabditis elegans*. *RNA* **12**, 589–597 (2006).
44. Duchaine, T.F. *et al.* Functional proteomics reveals the biochemical niche of *C. elegans* DCR-1 in multiple small-RNA-mediated pathways. *Cell* **124**, 343–354 (2006).
45. Pak, J. & Fire, A. Distinct populations of primary and secondary effectors during RNAi in *C. elegans*. *Science* **315**, 241–244 (2007).
46. Ruby, J.G. *et al.* Large-scale sequencing reveals 21U-RNAs and additional microRNAs and endogenous siRNAs in *C. elegans*. *Cell* **127**, 1193–1207 (2006).
47. Vagin, V.V. *et al.* A distinct small RNA pathway silences selfish genetic elements in the germline. *Science* **313**, 320–324 (2006).
48. Houwing, S. *et al.* A role for Piwi and piRNAs in germ cell maintenance and transposon silencing in Zebrafish. *Cell* **129**, 69–82 (2007).